Entanglement in interacting quenched two-body coupled oscillator system

Sayantan Choudhury[,1,*] Rakshit Mandish Gharat[,2,†] Saptarshi Mandal[,3,‡]
Nilesh Pandey,[4,§] Abhishek Roy,[5,∥] and Partha Sarker[6,¶]

[1]*International Centre for Theoretical Sciences, Tata Institute of Fundamental Research (ICTS-TIFR),
Shivakote, Bengaluru 560089, India*
[2]*Department of Physics, National Institute of Technology Karnataka, Surathkal, Karnataka-575025, India*
[3]*Department of Physics, Indian Institute of Technology Kharagpur, Kharagpur-721302, India*
[4]*Department of Applied Physics, Delhi Technological University, Delhi-110042, India*
[5]*Department of Physics, Indian Institute of Technology Jodhpur, Karwar, Jodhpur-342037, India*
[6]*Department of Physics, University of Dhaka, Curzon Hall, Dhaka 1000, Bangladesh*

In this work, we explore the effects of a quantum quench on the entanglement measures of a two-body coupled oscillator system having quartic interaction. We use the invariant operator method, under a perturbative framework, for computing the ground state of this system. We give the analytical expressions for the total and reduced density matrix of the system having non-Gaussian, quartic interaction terms. Using this reduced density matrix, we show the analytical calculation of two entanglement measures viz., Von Neumann entanglement entropy using replica trick and Renyi entanglement entropy. Further, we give a numerical estimate of these entanglement measures with respect to the dimensionless parameter $(t/\delta t)$ and show its behavior in the three regimes, i.e., late time behavior, around the quench point and the early time behavior. We comment on the variation of these entanglement measures for different orders of coupling strength. The variation of Renyi entropy of different orders has also been discussed.

I. INTRODUCTION

In recent years, the most important works in theoretical physics have been studied by blending the ideas of quantum many-body physics, quantum information theory and quantum field theory. The amalgamation of these branches of physics have been reviewed in [1–7]. These works mostly focus on studying the dynamical properties of quantum entanglement in time-dependent systems [8–17]. This dynamical entanglement can be characterized by computing von Neumann entanglement entropy and Renyi entanglement entropy. The traditional way of computing these entanglement measures involves constructing the reduced density matrix using the eigenstates of the time-dependent Hamiltonian.

*sayantan.choudhury@icts.res.in, sayanphysicsisi@gmail.com
†rakshitmandishgharat.196ph018@nitk.edu.in
‡saptarshijhikra@gmail.com
§nilesh911999@gmail.com
∥roy.1@iitj.ac.in
¶sarker239@gmail.com

One of the ways to compute the eigenstates of such time-dependent Hamiltonians is by constructing the Lewis-Resenfield invariant operator and this is often termed as invariant operator representation of the wave function [18]. Some works following this approach to compute the time-dependent eigenstates are [19–23]. Evolution of such time-dependent quantum states can be studied as a solution to the Ermakov-Milne-Pinney equation [24–26]. The invariant operator method is generalized for perturbed theories by computing time-independent perturbative corrections [27], considering adiabatic evolution [28,29] of the parameters.

For unperturbed Hamiltonians or free theories, the reduced density matrix once computed represents the Gaussian states. Entanglement can then be computed using these Gaussian states [30–32,32]. Computing von Neumann entropy for these Gaussian states employs the use of correlation functions defined using the framework of quantum field theory [33].

Entanglement in interacting theories has been studied using replica trick [34] in [35]. On the other hand, the perturbed entanglement entropy is computed using the path-integral approach in [36].

Most of the recent works in many-body physics have been about contemplating the behavior of entanglement for a system having a time-dependent parameter in

Hamiltonian. This time-dependent parameter can be varied quickly or slowly and hence the process is termed as a "quantum quench." Some of the most important works for studying entanglement-properties of extended systems undergoing a quantum quench are [37–46]. These quantum quenches can be thought of as protocols driving the system out-of-equilibrium [47–49]. These local equilibrium can then be analyzed in quenched systems by using reduced density matrix. In recent years, effects of quantum quenches have even been studied experimentally using cold atom systems [50–59]. Studying the effect of quantum quench in the case of interacting theories or perturbed theories is of prime importance [60].

In recent years, the study of coupled oscillators has been an area of active research. This is primarily due to the extensive use of such models in studying quantum and nonlinear physics [61–65], molecular chemistry [66–68] and biophysics [69–71]. Especially, in quantum physics, analyzing entanglement of coupled oscillators is of prime importance [72–76].

Motivated by the discussion given above, in this work we consider a toy model with a Hamiltonian of two coupled oscillators having quartic self-coupling term. The Hamiltonian for this system consists of a time-dependent quench profile. The eigenstates for this time-dependent Hamiltonian are computed using invariant operator method, in a perturbative framework. Further, the reduced density matrix (with quartic interaction terms) is constructed using time-independent perturbation theory. The dynamical von Neumann entropy and Renyi entropy are then derived using appropriate formulas for the obtained reduced density matrix. We comment on the behavior of these entanglement measures by varying the relevant parameters.

The organization of the paper is as follows:
(i) We start our discussion by providing an overview of the quench protocol and Hamiltonian of the system in Sec. II.
(ii) In Sec. III, the expression for eigenstates of the time-dependent Hamiltonian is computed using invariant-operator representation of wave function. Further, the expression for first order time-independent correction to the ground state of the Hamiltonian is also approximated in this section.
(iii) In Sec. IV, we use the ground state wave function with perturbative correction to compute the expression for reduced density matrix, with quartic interaction terms. von Neumann entanglement entropy is then computed by performing the replica trick over this reduced density matrix. Further, we show the analytically computed expression for Renyi entanglement entropy.
(iv) In Sec. V, we numerically evaluate the respective entanglement measures and plot them with respect to the dimensionless parameter $(t/\delta t)$. We comment on

the parametric variation of these entanglement measures for each of the chosen three regimes.
(v) Section VI summarizes the conclusions we draw from the obtained results of this work with some interesting future prospects of our present work.

II. THE SETUP AND THE QUENCH PROTOCOL

In this section we begin by discretizing the Hamiltonian for a scalar field theory with ϕ^4 interaction term on a lattice. We show that the Hamiltonian then represents a family of infinite anharmonic oscillators with quartic couplings. In this article, we study a system of two coupled oscillators having quartic perturbation. Furthermore, we use normal mode basis to decouple the Hamiltonian so that we can compute the eigenstates for this system in a much simpler way, in upcoming section. Also, we mention the time-dependent quench profile chosen as the frequency of this Hamiltonian.

The Hamiltonian for a scalar field theory with a $\hat{\lambda}\phi^4$ interaction is given by [77],

$$\mathcal{H} = \frac{1}{2}\int d^{d-1}x\left[\pi(x)^2 + (\nabla\phi(x))^2 + m^2\phi(x)^2 + \frac{\hat{\lambda}}{12}\phi(x)^4\right].$$
(1)

Here d is the space-time dimensions. We assume that the coupling $\hat{\lambda} \ll 1$, so that we can work in a perturbative framework. This theory can be discretized on a $d-1$ dimensional lattice, which is characterized by lattice spacing, δ. It can be shown that, the discretized Hamiltonian becomes,

$$\mathcal{H} = \frac{1}{2}\sum_{\vec{n}}\left\{\frac{\pi(\vec{n})^2}{\delta^{d-1}} + \delta^{d-1}\left[\frac{1}{\delta^2}\sum_i(\phi(\vec{n}) - \phi(\vec{n} - \hat{x}_i))^2\right.\right.$$
$$\left.\left. + m^2\phi(\vec{n})^2 + \frac{\hat{\lambda}}{12}\phi(\vec{n})^4\right]\right\}.$$
(2)

Here $\vec{n}$ denotes the spatial location of the points on lattice and $\hat{x}_i$ represent the unit vectors along the lattice. Further, we introduce the following substitutions to simplify the form of the Hamiltonian:

$$\hat{X}(\vec{n}) = \delta^{d/2}\phi(\vec{n}), \qquad \hat{P}(\vec{n}) = \pi(\vec{n})/\delta^{d/2},$$
$$M = \frac{1}{\delta}, \qquad \omega = m,$$
$$\eta = \frac{1}{\delta}, \qquad \lambda = \frac{\hat{\lambda}}{24}\delta^{-d},$$
(3)

where ω represents the frequency of individual oscillators and η denotes intermass coupling. After these substitutions we get,

$$\mathcal{H} = \sum_{\vec{n}} \left\{ \frac{\hat{P}(\vec{n})^2}{2M} + \frac{1}{2}M\left[\omega^2\hat{X}(\vec{n})^2 + \eta^2\sum_i(\hat{X}(\vec{n}) - \hat{X}(\vec{n} - \hat{x}_i))^2 \right. \right.$$
$$\left. \left. + 2\lambda\hat{X}(\vec{n})^4 \right] \right\}. \tag{4}$$

The above Hamiltonian, in Eq. (4) represents a family of infinite coupled anharmonic oscillators. In this work we focus on the system representing two coupled oscillators and compute the entanglement for this system. Setting $M = 1$, for simplicity, Eq. (4) can be specialized for case of two coupled oscillators,

$$H = \frac{1}{2}[p_1^2 + p_2^2 + \omega^2(x_1^2 + x_2^2) + \eta^2(x_1 - x_2)^2$$
$$+ 2\{\lambda(x_1^4 + x_2^4)\}]. \tag{5}$$

Here x_i and p_i, for $i = 1, 2$ denote the canonical coordinates of the respective oscillator following the standard commutation relation $[x_i, p_j] = i\delta_j^i$, while λ denotes the coupling coefficient of ϕ^4 interaction term.

The eigenstates of the above Hamiltonian Eq. (5), can easily be computed using normal coordinates defined as,

$$X_1 = (x_1 + x_2)/\sqrt{2}$$
$$X_2 = (x_1 - x_2)/\sqrt{2}$$
$$P_1 = (p_1 + p_2)/\sqrt{2}$$
$$P_2 = (p_1 - p_2)/\sqrt{2}. \tag{6}$$

The unperturbed part of Hamiltonian when written using these normal coordinates decouples. One can then show that the total Hamiltonian of Eq. (5) in normal coordinates takes the following form:

$$H = \sum_{i=1}^{2} H_i + H_p,$$

where,

$$H_i(T) = \frac{1}{2}(P_i^2 + \omega_i^2(T)X_i^2), \tag{7}$$

denotes the unperturbed and decoupled Hamiltonian for each of the two oscillators. On the other hand the perturbed Hamiltonian is given by,

$$H_p = \lambda V = \lambda(x_1^4 + x_2^4)$$
$$= \lambda(X_1^4 + X_2^4 + 6X_1^2X_2^2). \tag{8}$$

This enables us to use $\lambda\phi^4$ time-independent perturbation theory and compute the eigenstates of the total Hamiltonian of Eq. (5).

We now consider the frequency ω in, Eq. (5) as a time-dependent quench profile. One of the most common quench profiles used in literature [78,79] is given by:

$$\omega^2(t/\delta t) = \omega_0^2\left[\tanh^2\left(\frac{t}{\delta t}\right)\right]. \tag{9}$$

Here ω_0 can be interpreted as a free parameter and δt is the quench parameter or the quench rate. The quench profile chosen here is such that it admits an exact solution for the mode functions given in [79] and the quench profile attains a constant value at late and early times. The dynamical process due to this profile happens in the $[-\delta t, \delta t]$ time window. We will set $t/\delta t = T$ and $\omega_0 = 1$. The respective frequencies in normal mode basis take the following form,

$$\omega_1 = \omega(T) \quad \text{and} \quad \omega_2 = \sqrt{\omega^2(T) + 4\eta^2}, \tag{10}$$

where $\omega(T)$ is the quench profile Eq. (9).

Note that the unperturbed Hamiltonian of Eq. (7) is now time-dependent while the perturbed Hamiltonian of Eq. (8) acts as time-independent ϕ^4 coupling applied on the two harmonic oscillators. In Sec. III, we show the analytical computation of ground state, $\Psi_{0,0}$ of the total Hamiltonian of two coupled anharmonic oscillators having $\lambda\phi^4$ perturbation. This ground state is used to derive the analytical expressions of the respective entanglement measures in Sec. IV.

III. CONSTRUCTING WAVE FUNCTION FOR A ϕ^4 QUENCH MODEL

In this section our prime objective is to construct the wave function approximated to first order in coupling constant λ. In Sec. III A we compute the eigenstates of decoupled and unperturbed Hamiltonian Eq. (7). These eigenstates are then used to construct the ground state of perturbed Hamiltonian Eq. (8), approximated to first perturbative order, in Sec. III B. Finally we compute the total wave function as ground state of total Hamiltonian Eq. (5).

A. Eigenstates and eigenvalues for unperturbed Hamiltonian

As, the unperturbed Hamiltonian Eq. (7) decouples in the normal mode basis, the eigenstates for the unperturbed Hamiltonian are just the product of the eigenstates of respective oscillators in the normal-mode basis:

$$\psi_{n_1,n_2}^{(0)}(X_1, X_2, T) = \psi_{n_1}(X_1, T)\psi_{n_2}(X_2, T). \tag{11}$$

Since the unperturbed Hamiltonian consists of a time-dependent frequency scale, we now use a prescription often termed as the invariant representation in the literature [80], to get the unperturbed eigenstates.

We begin the invariant representation by listing the auxiliary equations. The solutions to these equations can

then be used to compute the coupled wave function. The auxiliary equations can be written as:

$$\ddot{\sigma}_j - \sigma_j \dot{\gamma}_j + \omega_j^2(T)\sigma_j = 0$$
$$\sigma_j \ddot{\gamma}_j + 2\dot{\sigma}_j \dot{\gamma}_j = 0. \tag{12}$$

Here, $j = 1, 2$ and $\sigma_j(T)$ and $\gamma_j(T)$ are time-dependent factors for each of the two coupled oscillators. Also, $\dot{\gamma}_j = \partial_T \gamma_j$, $\dot{\sigma}_j = \partial_T \sigma_j$ and $\ddot{\sigma}_j = \partial_T^2 \sigma_j$. The subscript j denotes the oscillator for which the respective parameter is mentioned. The computation of explicit values of $\sigma(T)$ and $\gamma(T)$ is discussed in Appendix A. Note that we have suppressed the time-dependence throughout this section. Next, we define the creation $(a_j^\dagger)$ and annihilation (a_j) operators given by,

$$a_j = \frac{1}{\sqrt{2\dot{\gamma}_j}} \left[\dot{\gamma}_j \left(1 - i\frac{\dot{\sigma}_j}{\sigma_j \dot{\gamma}_j} \right) X_j + iP_j \right]$$
$$a_j^\dagger = \frac{1}{\sqrt{2\dot{\gamma}_j}} \left[\dot{\gamma}_j \left(1 + i\frac{\dot{\sigma}_j}{\sigma_j \dot{\gamma}_j} \right) X_j - iP_j \right]. \tag{13}$$

Here, $j = 1, 2$. One can show that these operators satisfy the commutation relation $[a_i, a_j^\dagger] = \delta_j^i$. The creation and annihilation operators can be used to define invariant operator for the respective decoupled Hamiltonian,

$$I_j = \Omega_j \left(a_j^\dagger a_j + \frac{1}{2} \right). \tag{14}$$

Here, $j = 1, 2$. On the other hand, $\Omega_j = \sigma_j^2 \dot{\gamma}_j$, is an invariant quantity with respect to time. The construction of this invariant operator Eq. (14) has been briefly outlined in Appendix B. The invariant operator has its own spectrum and eigenstates. The eigenstates of invariant operator can be used to formulate the wave functions for each decoupled Hamiltonian. The outline of the same is given in Appendix B. Using equation (B4) for n_1, $n_2 = 0$, one can show that the ground state of unperturbed Hamiltonian is given by,

$$\psi_{0,0}^{(0)} = \sqrt{\frac{g_1 g_2}{\pi}} \exp\left[-i\frac{\gamma_1 + \gamma_2}{2} \right]$$
$$\times \exp\left[-\frac{1}{2}(g_1^2(1 - id)X_1^2 + g_2^2(1 - if)X_2^2) \right]. \tag{15}$$

where, the coefficients g_1, g_2, d, and f are given by,

$$g_1 = \sqrt{\dot{\gamma}_1}, \quad g_2 = \sqrt{\dot{\gamma}_2}, \quad d = \frac{\dot{\sigma}_1}{\dot{\gamma}_1 \sigma_1}, \quad f = \frac{\dot{\sigma}_2}{\dot{\gamma}_2 \sigma_2}. \tag{16}$$

Next we emphasize that the eigenvalues of the unperturbed decoupled Hamiltonians in Eq. (7) will have a time dependent factor [27]. These eigenvalues for each of the decoupled Hamiltonians are given as:

$$\langle \psi_{n_j} | H_i | \psi_{n_j} \rangle = W_j(T)\left[n_j + \frac{1}{2} \right], \tag{17}$$

where, $j = 1, 2$. Here $W_j(T)$ is the time-dependent factor for each oscillator given by,

$$W_j(T) = \frac{\dot{\gamma}_j}{2} \left(\frac{\dot{\sigma}_i + \sigma_i^2 \omega_i^2 + \sigma_i^2 \dot{\gamma}_i}{\sigma_i^2 \dot{\gamma}_i^2} \right), \tag{18}$$

where $j = 1, 2$. Using the above eigenvalues one can write the energy eigenvalue for the unperturbed state of two coupled oscillators, Eq. (B4) as:

$$\langle \psi_{n_1,n_2}^{(0)} | H | \psi_{n_1,n_2}^{(0)} \rangle = W_1(T)\left(n_1 + \frac{1}{2} \right) + W_2(T)\left(n_2 + \frac{1}{2} \right). \tag{19}$$

B. Ground state of two coupled oscillators with first order-ϕ^4 perturbation

Using time-independent perturbation theory, one can show that the first order perturbative correction to the ground state of two-coupled oscillators is,

$$\psi_{0,0}^{(1)} = \sum_{(n_1,n_2)\neq(0,0)} \frac{\langle \psi_{n_1,n_2}^{(0)} | V | \psi_{0,0}^{(0)} \rangle \times \psi_{n_1,n_2}^{(0)}.}{\langle \psi_{0,0}^{(0)} | H | \psi_{0,0}^{(0)} \rangle - \langle \psi_{n_1,n_2}^{(0)} | H | \psi_{n_1,n_2}^{(0)} \rangle} \tag{20}$$

Using the form of perturbed Hamiltonian Eq. (8) and the time dependent eigenvalues Eq. (19), the above expression when evaluated becomes,

$$\psi_{0,0}^{(1)} = -\frac{3(g_1^2 + g_2^2)\psi_{0,2}^{(0)}}{4\sqrt{2}hg_1^2 g_2^2} - \frac{3\psi_{0,4}^{(0)}}{8\sqrt{2}hg_2^2} - \frac{3(g_1^2 + g_2^2)\psi_{2,0}^{(0)}}{4\sqrt{2}gg_1^2 g_2^2}$$
$$- \frac{3\psi_{2,2}^{(0)}}{2(2g + 2h)2g_1^2 g_2^2} - \frac{3\psi_{4,0}^{(0)}}{8\sqrt{2}gg_1^2}. \tag{21}$$

Here,

$$g = \left(\frac{\dot{\sigma}_1 + \sigma_1^2 \omega_1^2 + \Omega_1 \dot{\gamma}_1}{\Omega_1} \right),$$
$$h = \left(\frac{\dot{\sigma}_2 + \sigma_2^2 \omega_2^2 + \Omega_2 \dot{\gamma}_2}{\Omega_2} \right). \tag{22}$$

The explicit form of the first order correction can be computed using the expression of unperturbed eigenstates, Eq. (B4). The total wave function for ground state of total Hamiltonian Eq. (5), corrected to first order of time-independent $\lambda\phi^4$ perturbation, is given by: $\Psi_{0,0} = \psi_{0,0}^{(0)} + \lambda\psi_{0,0}^{(1)}$. Using Eq. (15) and Eq. (21) while approximating, the coupling constant $\lambda \ll 1$ we can express the final form of the wave function in normal mode basis as:

$$\Psi_{0,0}(X_1, X_2) = \left(\frac{g_1^2 g_2^2}{\pi^2}\right)^{\frac{1}{4}} e^{-i\frac{(\gamma_1+\gamma_2)}{2}} \exp\left[-\frac{1}{2}(1-id)g_1^2 X_1^2 - \frac{1}{2}(1-if)g_2^2 X_2^2 + \lambda(A_1 + A_2 X_1^2 + A_3 X_2^2 + A_4 X_1^4 + A_5 X_2^4 + A_6 X_1^2 X_2^2)\right].$$

(23)

The coefficients A_i for $i = 1$ to $i = 6$ are mentioned in a table given in Appendix D. The above wave function Eq. (23) represents the ground state of total Hamiltonian in Eq. (5), of the system of two coupled oscillators with $\lambda\phi^4$ perturbation. We take note of the fact that all variables, aside from the coordinates, X_1, X_2 and coupling constant, λ in the wave function, Eq. (23) are functions of timescale T. The wave function is then dependent on both t and δt. This explicit time dependence can be evaluated by computing σ_i and γ_i, shown in Appendix A.

IV. ANALYTICAL CALCULATION OF ENTANGLEMENT MEASURES

In the previous Secs. II and III, we computed the ground state wave function for a system of two coupled bosonic oscillators with a ϕ^4 first-order perturbative correction for Hamiltonian having a quenched frequency-profile. In this section our prime objective is to show the analytical steps to calculate entanglement measures, viz., von Neumann entanglement entropy and Renyi entropy.

In Sec. IV A reduced density matrix for the system of two coupled oscillators is constructed using the wave function

Eq. (23). To compute von Neumann entropy using replica trick [34,35] as well as Renyi entropy, the trace of reduced density matrix should be evaluated, this is shown in Sec. IV B. Finally using the appropriate formulas we show the computation of the respective entanglement measures in Sec. IV C.

A. Density matrix for perturbed wave function

We begin by transforming the wave function $\Psi(X_1, X_2)$ given in Eq. (23) to $\Psi(x_1, x_2)$, i.e., we transform the normal coordinates back to space-time coordinates using Eq. (6). We mention four new symbols:

$$P = \frac{1}{2}(1-id)g_1^2; \qquad P^* = \frac{1}{2}(1+id)g_1^2$$

$$Q = \frac{1}{2}(1-if)g_2^2; \qquad Q^* = \frac{1}{2}(1+if)g_1^2. \qquad (24)$$

The wave function in spacetime coordinates is then represented by:

$$\Psi(x_1, x_2) = \left(\frac{g_1^2 g_2^2}{\pi^2}\right)^{\frac{1}{4}} e^{-i(\gamma_1+\gamma_2)/2} \exp\left\{-\frac{P}{2}(x_1^2 + x_2^2 + 2x_1 x_2) - \frac{Q}{2}(x_1^2 + x_2^2 - 2x_1 x_2) + \lambda\left[A_1 + \frac{A_2}{2}(x_1^2 + x_2^2 + 2x_1 x_2)\right.\right.$$

$$+ \frac{A_3}{2}(x_1^2 + x_2^2 - 2x_1 x_2) + \frac{A_4}{4}(x_1^4 + x_2^4 + 4x_1^3 x_2 + 4x_1 x_2^3 + 6x_1^2 x_2^2)$$

$$\left.\left. + \frac{A_5}{4}(x_1^4 + x_2^4 - 4x_1^3 x_2 - 4x_1 x_2^3 + 6x_1^2 x_2^2) + \frac{A_6}{4}(x_1^4 + x_2^4 - 2x_1^2 x_2^2)\right]\right\}.$$

(25)

The complex conjugate of the above given wave function is denoted by $\Psi^*(x_1', x_2')$. Using the conjugate of the wave function in Eq. (25), we can construct the total density matrix for the system of two oscillators by $\rho(x_1, x_2, x_1', x_2') = \Psi(x_1, x_2)\Psi^*(x_1', x_2')$. One can easily show that the density matrix is given as:

$$\rho(x_1, x_2, x_1', x_2') = \left(\frac{g_1 g_2}{\pi}\right) \exp\left\{-\frac{P}{2}(x_1^2 + x_2^2 + 2x_1 x_2) - \frac{P^*}{2}(x_1'^2 + x_2'^2 + 2x_1' x_2') - \frac{Q}{2}(x_1^2 + x_2^2 - 2x_1 x_2) - \frac{Q^*}{2}(x_1'^2 + x_2'^2 - 2x_1' x_2')\right.$$

$$+ \lambda\left[2A_1 + \frac{A_2}{2}(x_1^2 + x_1'^2 + x_2^2 + x_2'^2 + 2x_1 x_2 + 2x_1' x_2') + \frac{A_3}{2}(x_1^2 + x_1'^2 + x_2^2 + x_2'^2 - 2x_1 x_2 - 2x_1' x_2')\right.$$

$$+ \frac{A_4}{4}(x_1^4 + x_1'^4 + x_2^4 + x_2'^4 + 4x_1^3 x_2 + 4x_1'^3 x_2' + 4x_1 x_2^3 + 4x_1' x_2'^3 + 6x_1^2 x_2^2 + 6x_1'^2 x_2'^2)$$

$$+ \frac{A_5}{4}(x_1^4 + x_1'^4 + x_2^4 + x_2'^4 - 4x_1^3 x_2 - 4x_1'^3 x_2' - 4x_1 x_2^3 - 4x_1' x_2'^3 + 6x_1^2 x_2^2 + 6x_1'^2 x_2'^2)$$

$$\left.\left. + \frac{A_6}{4}(x_1^4 + x_1'^4 + x_2^4 + x_2'^4 - 2x_1^2 x_2^2 - 2x_1'^2 x_2'^2)\right]\right\}.$$

(26)

The reduced density matrix can be computed using total density matrix, shown in Eq. (26) by tracing over the coordinates of second oscillator, i.e., by setting $x_2' = x_2$ and computing $\rho(x_1, x_1', x_2)$. The reduced density matrix can then be evaluated as:

$$\rho(x_1, x_1') = \int_{-\infty}^{\infty} \rho(x_1, x_1', x_2) dx_2. \tag{27}$$

We mention the final form of the reduced density matrix which can be used to calculate the entanglement measures as:

$$\rho(x_1, x_1') = N\left(\frac{g_1 g_2}{\pi}\right)\sqrt{\frac{\pi}{A}}\exp\left\{(2\lambda A_1 + \lambda\alpha_0) + \left(\frac{-(P+Q)}{2} + \frac{(Q-P)^2}{4A} + \lambda\alpha_1\right)x_1^2 + \left(\frac{-(P^*+Q^*)}{2} + \frac{(Q^*-P^*)^2}{4A} + \lambda\alpha_2\right)x_1'^2\right.$$
$$\left. + \left(\frac{(Q-P)(Q^*-P^*)}{2A} + \lambda\alpha_3\right)x_1 x_1' + \lambda[\alpha_4 x_1^4 + \alpha_5 x_1'^4 + \alpha_6 x_1^3 x_1' + \alpha_7 x_1 x_1'^3 + \alpha_8 x_1^2 x_1'^2]\right\}. \tag{28}$$

Here N is the normalization factor, while,

$$A = \left(\frac{g_1^2 + g_2^2}{2}\right)$$

$$B = ((Q-P)x_1 + (Q^*-P^*)x_1'). \tag{29}$$

The values of coefficients, α_i for $i = 0$ to $i = 8$, are listed in Appendix D.

B. Computing the value of $tr(\rho^n)$

In this subsection we outline analytical steps to compute the expression for $tr(\rho^n)$ where ρ is the reduced density matrix of Eq. (28). The reduced density matrix, given by Eq. (28) is clearly representing a non-Gaussian state. The

calculation of entanglement entropy for such a non-Gaussian state is shown in [35]. We follow a similar method and modify the same derivation to compute entropy for the state representing Eq. (28).

According to the definition of trace, considering that $x_{n+1} = x_1$, one can write:

$$tr(\rho^n) = \int dx_1 dx_2 \cdots dx_n \rho(x_1, x_2)\rho(x_2, x_3) \cdots \rho(x_n, x_1), \tag{30}$$

where, $\rho(x_i, x_{i+1})$, for $i = 1$ to n, represents the reduced density matrix given in Eq. (28). The product of density matrices in Eq. (30), when evaluated gives:

$$tr(\rho^n) = N^n\left(\frac{g_1 g_2}{\pi}\right)^n\left(\sqrt{\frac{\pi}{A}}\right)^n e^{n(2\lambda A_1 + \lambda\alpha_0)}\int d^n x \exp\left\{\left[\frac{-(P+P^*+Q+Q^*)}{2} + \frac{(Q-P)^2 + (Q^*-P^*)^2}{4A} + \lambda(\alpha_1 + \alpha_2)\right]\sum_{i=1}^{n} x_i^2\right.$$
$$\left. + \left[\frac{(Q-P)(Q^*-P^*)}{2A} + \lambda\alpha_3\right]\sum_{i=1}^{n} x_i x_{i+1} + \lambda\left[(\alpha_4 + \alpha_5)\sum_{i=1}^{n} x_i^4 + (\alpha_6 x_{i-1}^3 + \alpha_7 x_{i+1}^3)\sum_{i=1}^{n} x_i + \alpha_8\sum_{i=1}^{n} x_i^2\sum_{i=1}^{n} x_{i+1}^2\right]\right\}. \tag{31}$$

We modify the above expression by using new coefficients $\beta_1, \beta_2 \ldots \beta_7$ tabulated in Appendix D. Note that each β_i for $i = 1$ to 7 is evaluated by substituting P, Q, A, and B defined in Eq. (24) and Eq. (29). One can then show that,

$$tr(\rho^n) = N^n\left(\frac{g_1 g_2}{\pi}\right)^n\left(\sqrt{\frac{\pi}{A}}\right)^n e^{n(2\lambda A_1 + \lambda\alpha_0)}\int d^n x \left\{\exp\left[(\beta_1 + \lambda\beta_2)\sum_{i=1}^{n} x_i^2 + (\beta_3 + \lambda\beta_4)\sum_{i=1}^{n} x_i x_{i+1}\right]\right.$$
$$\left. \times \exp\left\{\lambda\left[\beta_5\sum_{i=1}^{n} x_i^4 + (\alpha_6 x_{i-1}^3 + \alpha_7 x_{i+1}^3)\sum_{i=1}^{n} x_i + \beta_6\sum_{i=1}^{n} x_i^2\sum_{i=1}^{n} x_{i+1}^2\right]\right\}\right\}. \tag{32}$$

The integral in the above Eq. (32) can be solved using the steps shown in Appendix C.

To evaluate normalization factor N one needs to set $tr(\rho(x_1, x_1')) = 1$ for the reduced density matrix in Eq. (28). Using μ and ξ defined in Appendix C the normalization factor is given by,

$$N^n = \left(\frac{g_1 g_2}{\pi}\right)^{-n}\left(\sqrt{\frac{\pi}{A}}\right)^{-n} e^{-n(2\lambda A_1 + \lambda\alpha_0)}\left(\frac{\beta}{\pi}\right)^{\frac{n}{2}}|1-\mu|^n\left(1 - \frac{3\lambda(\beta_5 + \beta_6 + \beta_7)}{4\beta^2(1-\mu)^4}\right)^n. \tag{33}$$

Substituting (33) and Eq. (C8) in Eq. (C12) from Appendix C, one can obtain the final value of trace of nth order of the reduced density matrix of Eq. (28), as:

$$tr(\rho^n) = \frac{|1-\mu|^n}{|1-\mu^n|}\left(1-\frac{3\lambda(\beta_5+\beta_6+\beta_7)}{4\xi^2(1-\mu)^4}\right)^n\{1+n\lambda[3\beta_5(M_{11}^{-1})^2+\beta_6(M_{11}^{-1})^2+2(M_{12}^{-1})^2+3\beta_7(M_{11}^{-1}M_{12}^{-1})]\}. \quad (34)$$

C. Entanglement measures

In this subsection we compute the two entanglement measures, viz., von Neumann entanglement entropy and Renyi entropy using the respective formulas for the reduced density matrix of Eq. (28).

The von Neumann entanglement entropy for a given density matrix ρ is computed as, $S_{VN} = -tr(\rho \ln \rho)$. As we know the explicit $n-$ dependence of $tr(\rho^n)$ from Eq. (34), we instead use replica trick often given as [34],

$$S_{VN} = -\lim_{n\to 1}\frac{\partial}{\partial n}tr(\rho^n). \quad (35)$$

Substituting the respective values of matrix inverses of, Eq. (C13) in Eq. (34) one can show that the von Neumann entropy is given by,

$$S_{VN} = -\frac{\mu\ln\mu+(1-\mu)\ln(1-\mu)}{(1-\mu)}+\lambda\left[\frac{3\mu\ln\mu}{\xi^2(\mu+1)(\mu-1)^5}\beta_5+\frac{\ln\mu(1+\mu+\mu^2)}{\xi^2(\mu+1)(\mu-1)^5}\beta_6+\frac{3\ln\mu(1+\mu)}{4\xi^2(\mu-1)^5}\beta_7\right]. \quad (36)$$

Using Eq. (C2), the above expression for von Neumann entropy can be approximated to first order in coupling constant λ as,

$$S_{VN} = -\frac{C_1\ln C_1+(1-C_1)\ln(1-C_1)}{(1-C_1)}+\lambda\left[-\frac{C_1C_2\ln C_1}{(1-C_1)^2}-\frac{C_2\ln C_1}{(1-C_1)}+\frac{3C_1\ln C_1}{C_3^2(C_1+1)(C_1-1)^5}\beta_5\right.$$
$$\left.+\frac{\ln C_1(1+C_1+C_1^2)}{C_3^2(C_1+1)(C_1-1)^5}\beta_6+\frac{3\ln C_1(1+C_1)}{4C_3^2(C_1-1)^5}\beta_7\right]. \quad (37)$$

The Renyi entropy of order n can be evaluated using,

$$S_R = \frac{1}{1-n}\ln[tr(\rho^n)]. \quad (38)$$

Substituting the respective values of matrix inverses, Eq. (C13) in Eq. (34) while using Eq. (C2) one can show that the Renyi entropy is given by,

$$S_R = \frac{1}{1-n}\left\{n\ln(1-C_2-\lambda C_3)-\ln(1-(C_2+\lambda)^n)+n\lambda\left[\left(-\frac{3}{4C_3^2(1-C_1)^4}+\frac{(C_1^{2n}-1)^2}{4C_3^2(1-C_1^n)^4(C_1^2-1)^2}\right)\beta_5\right.\right.$$
$$+\left(-\frac{3}{4C_3^2(1-C_1)^4}+\frac{(C_1^{2n}-1)^2}{4C_3^2(1-C_1^n)^4(C_1^2-1)^2}+2\frac{(C_1^n+C_1^2)^2}{4C_1^2C_3^2(C_1^2-1)^2(C_1^n-1)^2}\right)\beta_6$$
$$\left.\left.+\left(-\frac{3}{4C_3^2(1-C_1)^4}+\frac{3(C_1^{2n}-1)(C_1^n+C_1^2}{4C_1C_3^2(1-C_1^n)^2(C_1^2-1)^2(C_1^n-1)}\right)\beta_7\right]\right\}. \quad (39)$$

Note that the coefficients C_i for $i = 1, 2, 3, 4$ in Eq. (37) and Eq. (39) arise due to the analytical steps shown in Appendix C. These coefficients are tabulated in Appendix D.

Using the values of von Neumann entropy, Eq. (37) and Renyi entropy, Eq. (39) one can verify, using first order approximation in coupling constant λ,

$$\lim_{n\to 1}S_R = S_{VN}.$$

Note that the final formulas of von Neumann as well as Renyi entropies depend on β_i for $i = 1, 2...7$. These coefficients β_i, given in the table of IV B depend on timescale t and δt. Entanglement measures therefore depend on these timescales. We check this time-dependence by computing numerical values of both entanglement measures in section V.

V. NUMERICAL RESULTS

In this section we numerically evaluate von Neumann and Renyi entanglement entropy measures computed for the quench setup of two coupled oscillators using Eq. (37) and Eq. (39). As mentioned before each factor in the derived formulas for entanglement measures explicitly depends on $\sigma_i(t, \delta t)$ and $\gamma_i(t, \delta t)$. The values of $\sigma_i(t, \delta t)$ and $\gamma_i(t, \delta t)$ are computed by solving auxiliary equations, shown in, Eq. (12) which is outlined in Appendix A. Analytically solving the differential equation of Eq. (A1), is very complicated and hence we set some initial conditions to numerically evaluate the solution to this equation.

We begin by considering the coupling coefficient in the Hamiltonian of the coupled oscillators, Eq. (5) as $\eta = 0.5$. We further set the invariant quantities in Eq. (14) as, $\Omega_1 = \Omega_2 = 1$. To obtain the constants A, B, and C mentioned in Eq. (A4) we first compute $\sigma_i(t, \delta t)$ and $\gamma_i(t, \delta t)$ at $t \to 0$. Next we, set $d(t \to 0) = f(t \to 0) = 0$, defined in, Eq. (16) and $\sigma_i(0, \delta t) = 1$.

Using these initial conditions we obtain values of A, B, and C which can be inserted in Eq. (A4). $\rho_i(t, \delta t)$ and $\gamma_i(t, \delta t)$ are then used to get numerical values of von Neumann and Renyi entanglement entropies, for the aforementioned initial conditions. Using the numerical values of S_{VN} and S_R, we parametrize four different plots for a chosen timescale. We have varied the dimensionless

parameter $(t/\delta t)$ from 0.1 to 0.7 in steps of 0.05. The ratio is then plotted on the x-axis of the respective figures. We term the value of $(t/\delta t) = 1$ as the "quench point" represented by a red dotted line in all the respective figures. Using the values of $(t/\delta t)$ we divide all the plots in three different regions. The first region shaded as red, is marked for values of $(t/\delta t) < 0.8$. This region shows the "early-time behavior" of the respective entanglement measures, when the quench rate δt is varied in a way so as to keep $(t/\delta t) \ll 1$. The next region, shaded as yellow is marked by two equal intervals to the right as well as left of quench point, precisely for values of $(t/\delta t)$ between 0.8 and 1.2. This region represents the values of entanglement measures for $(t/\delta t) \approx 1$ and hence is termed as the region "around the quench point." The last region shaded as blue is marked for values of $(t/\delta t) > 1.2$. This region shows the "late-time behavior" of the respective entanglement measures, when the quench rate δt is varied in a way so as to keep $(t/\delta t) \gg 1$.

In Fig. 1 we have plotted the von Neumann (V-N) entropy for two coupled oscillators having quartic self-coupling with respect to the dimensionless parameter $(t/\delta t)$ for different orders of λ. We observe that the computed values of V-N entropy are negative for the chosen timescale for $\lambda > 10^{-5}$. We begin by plotting the values of V-N entropy by decreasing the order of λ, starting from
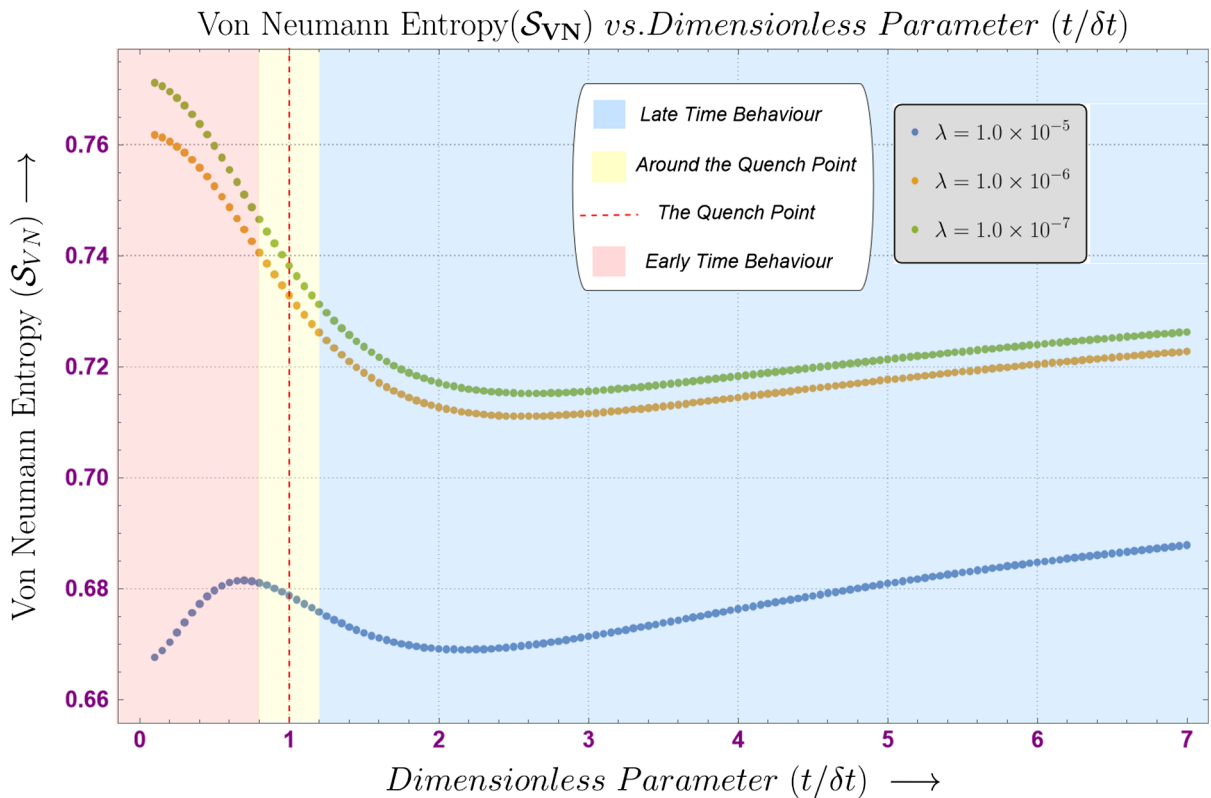

FIG. 1.   Variation of the Von Neumann entropy (S_{VN}) with respect to the dimensionless parameter $(t/\delta t)$ for different orders of the coupling constant λ for two coupled oscillators with quartic perturbation.

$\lambda = 10^{-5}$. We see that for $\lambda = 10^{-5}$ initially the V-N entropy grows for very small values of $(t/\delta t) < 0.6$. It can therefore be inferred from the plot that V-N entropy (for $\lambda = 10^{-5}$) increases in most of the region covering the early-time behavior, shaded as blue. Further, in the range $0.6 < (t/\delta t) < 2.2$ the entropy decreases gradually. Thus, the whole region near to the quench-point, shaded as yellow, shows a decreasing value of V-N entropy. After $(t/\delta t) > 2.2$ the V-N entropy increases monotonically and shows a thermalizing behavior for large values of $(t/\delta t)$. Most of the late-time behavior therefore, shows thermalizing behavior of V-N entropy.

In case of $\lambda = 10^{-6}$ and $\lambda = 10^{-7}$ we observe from the plot in Fig. 1, that there is a decrease in von Neumann entropy up to $(t/\delta t) < 2.6$. Hence, the whole early-time behavior region as well as the region around the quench point, shaded as red and yellow respectively, show a decreasing trend in V-N entropy. This trend is in contrast to the same for $\lambda = 10^{-5}$. When we move further toward larger values of the dimensionless parameter $(t/\delta t)$ we again see a thermalizing behavior for both the coupling constants. This region is shaded as blue and shows trend similar to that of $\lambda = 10^{-5}$. Another observation which we can make from this graph is that as we decrease the order of the coupling constant λ the von Neumann entropy increases.

In Fig. 2 we have plotted the Renyi entropies for two coupled oscillators having quartic self-coupling with respect to the dimensionless parameter $(t/\delta t)$ for different orders of λ. We observe that the computed values of Renyi entropy are negative for the chosen timescale for $\lambda > 10^{-4}$. We begin by plotting the values of Renyi entropy by decreasing the order of coupling constant, starting from $\lambda = 10^{-4}$. We see that for $\lambda = 10^{-4}$, initially the Renyi entropy grows for very small value of $(t/\delta t) < 0.8$. Hence, the early time-behavior of the system shows an increasing trend in values of Renyi entropy, shaded by red color. Further, in the range $0.8 < (t/\delta t) < 2.2$ the entropy decreases gradually. The region around the quench point, shaded as yellow, shows decreasing trend in Renyi entropy. After $(t/\delta t) > 2.2$ the Renyi entropy increases monotonically and shows a thermalizing behavior for large values of $(t/\delta t)$. Most of the late-time behavior of the system shows the thermalization trend in Renyi entropy. This region is shaded by blue color. This behavior is similar to that of V-N entropy for $\lambda = 10^{-5}$ shown in Fig. 1.

In case of $\lambda = 10^{-5}$ and $\lambda = 10^{-6}$ we observe from the graph that there is a decrease in Renyi entropy up to $(t/\delta t) < 2.6$. Hence, the early-time behavior as well as behavior of the system around the quench point results in decreasing values of Renyi entropy, shaded as red and yellow respectively in the Fig. 2. This trend is in contrast to
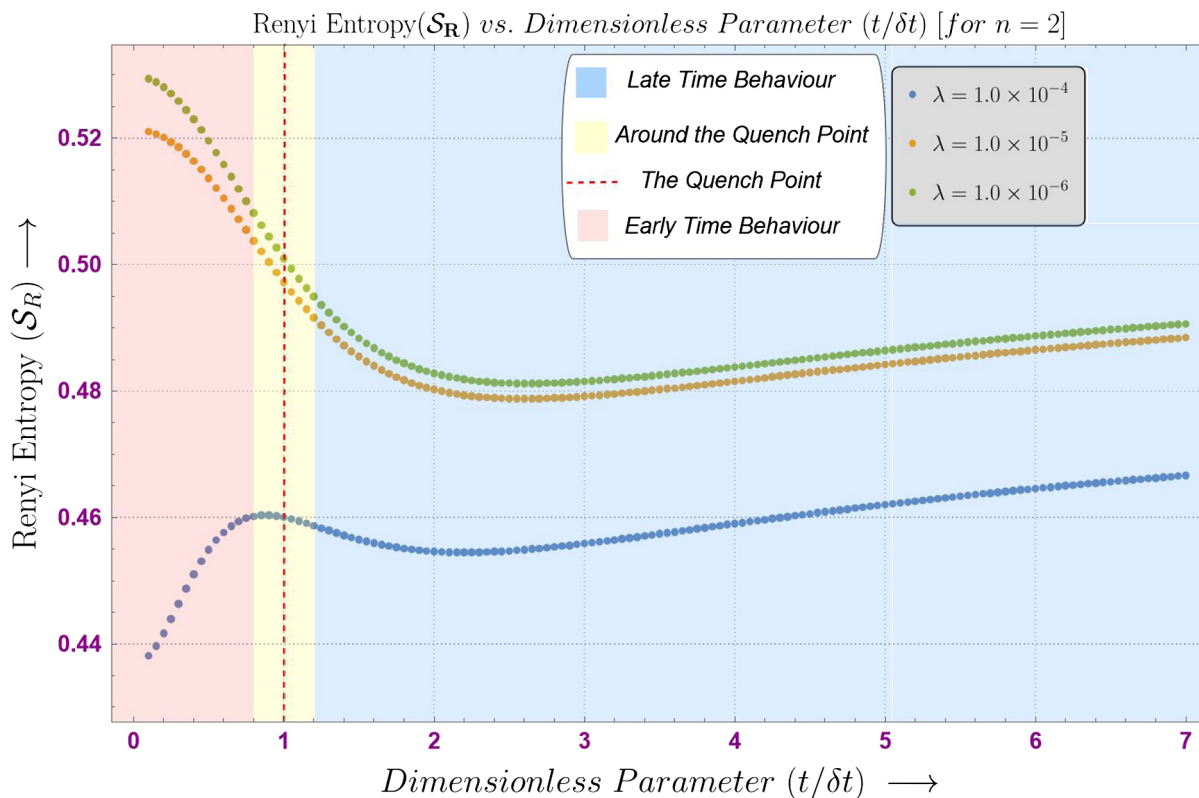

FIG. 2. Variation of the Renyi entropy (S_R) for $n = 2$, with respect to the dimensionless parameter $(t/\delta t)$ for different orders of the coupling constant λ for two coupled oscillators with quartic perturbation.
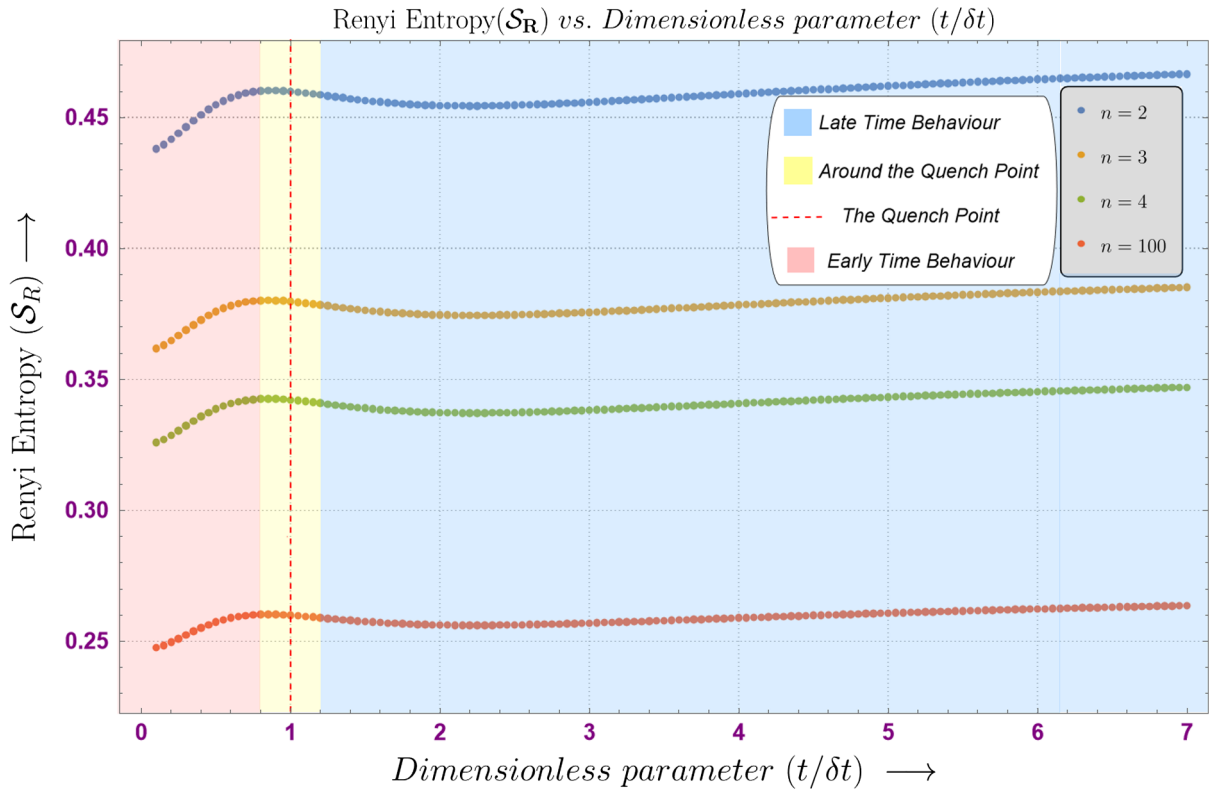
Renyi Entropy($\mathcal{S}_{\mathbf{R}}$) *vs. Dimensionless parameter* ($t/\delta t$)

FIG. 3. Variation of the Renyi entropy (S_R) for $\lambda = 10^{-4}$, with respect to the dimensionless parameter ($t/\delta t$) for different values of n for two coupled oscillators with quartic perturbation.

Renyi Entropy($\mathcal{S}_{\mathbf{R}}$) *vs. Dimensionless parameter* ($t/\delta t$)

FIG. 4. Variation of the Renyi entropy (S_R) for $\lambda = 10^{-5}$, with respect to the dimensionless parameter ($t/\delta t$) for different values of n for two coupled oscillators with quartic perturbation.
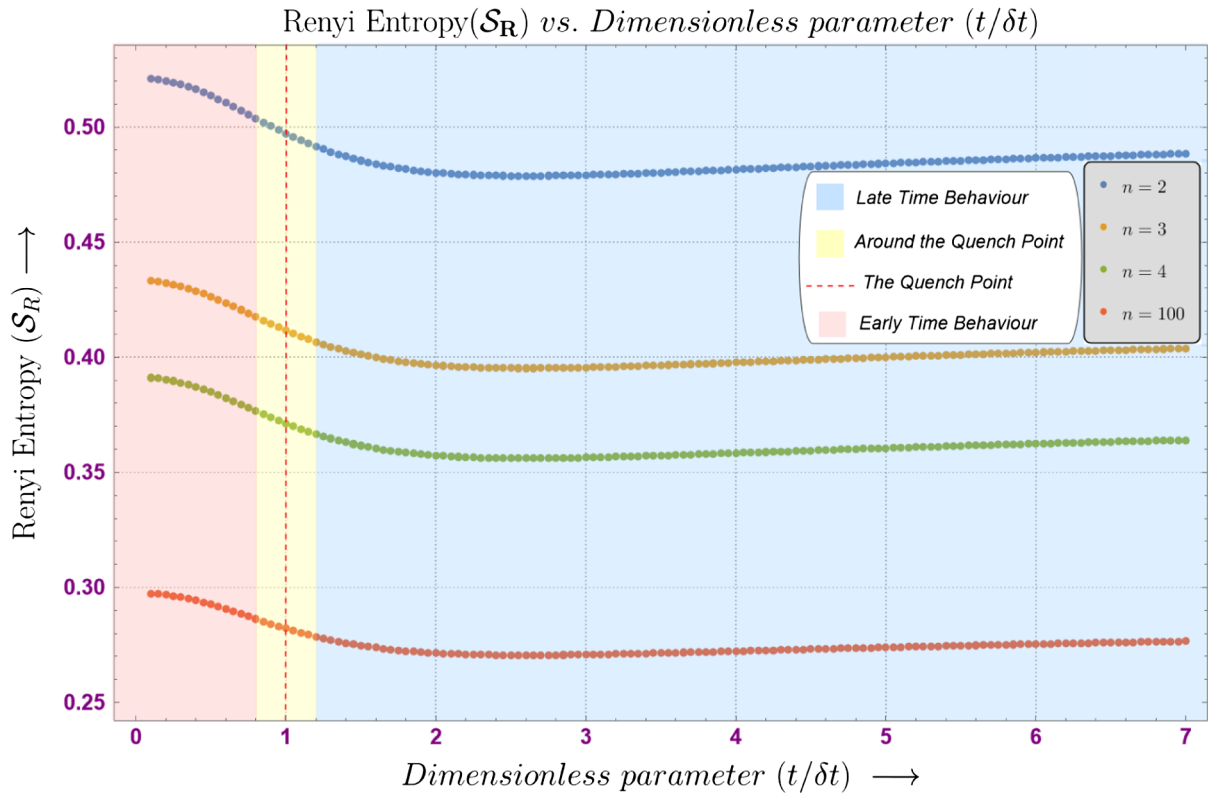
that of $\lambda = 10^{-4}$. When we move further toward larger values of the dimensionless parameter $(t/\delta t)$ we again see a thermalizing behavior for both the coupling constants. The late-time behavior of the system is, mostly characterized by thermalization of Renyi entropy. This is shown by blue region in Fig. 2. This behavior is similar to that of V-N entropy for $\lambda = 10^{-6}, 10^{-7}$ in Fig. 1. Another observation which we can make from this graph is that as we decrease the order of the coupling constant λ the Renyi entropy increases.

Hence, as we are decreasing the order of λ the plots of von Neumann entropy and that of Renyi entropy show a similar behavior with respect to each other, given that the order of λ in the case of von Neumann entropy is one lower than that in Renyi entropy.

In the Fig. 3 we have plotted the Renyi entropies for two coupled oscillators having quartic self-coupling with respect to the dimensionless parameter $(t/\delta t)$ for different orders of Renyi entropy, i.e., for different values of n, set at $\lambda = 10^{-4}$. The early time behavior shows an increasing trend in the value of Renyi entropy for the chosen values of $n = 2, 3, 4$. The entropy then decreases covering the region around the quench. Most of the late time behavior of the system shows thermalizing nature of Renyi entropy. It is clear that this scaling behavior is retained for large value of $n = 100$.

Figure 4 shows parametric variation for different orders of Renyi entropy, i.e., for different values of n, set at $\lambda = 10^{-5}$. The early time behavior as well as the behavior of system near the quench point, shows a decreasing trend in values of Renyi entropy. Most of the late-time behavior is characterized again by thermalization of Renyi entropy for chosen values of $n = 2, 3, 4$. Again, this scaling behavior is retained for large value of $n = 100$.

VI. CONCLUSION

The concluding remarks of this work are appended below pointwise:

(i) Focusing on a system of two coupled oscillators with quartic perturbation, we have derived analytical expressions of von Neumann entanglement entropy and Renyi entropy, undergoing a quantum quench.

(ii) First we have computed the expression for eigenstates of unperturbed Hamiltonian using invariant operator method. Using this expression we have approximated the first order $\lambda\phi^4$ correction for the total Hamiltonian of the system. Since the Hamiltonian is time-dependent due to the chosen quench profile as the frequency of the oscillators, it is quite evident that the total Hamiltonian can be quantized by using solutions to the Ermakov-Milne-Pinney equation. The ground state of the total Hamiltonian of the system, having ϕ^4 interaction term, is then used to derive analytical expressions for the respective entanglement measure.

(iii) Next we have mentioned the reduced density matrix for the ground state of the above described system of coupled oscillators. This reduced density matrix, clearly represents non-Gaussian state due to presence of quartic interaction terms. We deal with this non-Gaussian terms by constructing a quartic tensor and computing the trace of nth order of reduced density matrix.

(iv) Finally, we employ the use of replica trick for computing von Neumann entanglement entropy. Further, Renyi entropy was computed using the standard formula, depending on the reduced density matrix. The analytical expression for these entanglement measures is time-dependent as all the coefficients in the respective expression depend on solutions of Ermakov-Milne-Pinney equation.

(v) Using the numerically evaluated values of von Neumann entropy and Renyi entropy we studied the variation of these entanglement measures with respect to the dimensionless parameter $(t/\delta t)$ specifying three regions: early-time behavior, the behavior around the quench point and the late-time behavior.

(vi) From these numerical results, we find that both von Neumann entropy and Renyi entropy delicately depend on the order of coupling constant λ. Evidently there exists a respective threshold order of λ beyond which λ if increased, we do not get positive values of both von Neumann and Renyi entanglement entropies, for chosen values of $(t/\delta t)$. For the respective threshold order of λ we observe same scaling behavior in both von Neumann entropy and Renyi entropy. This scaling behavior can be characterized by a trend of increasing values of the entanglement measure for early times while in the region around the quench point the behavior shows a decreasing trend in these values.

(vii) As the order of λ is decreased below the respective threshold order we get another scaling behavior of both von Neumann and Renyi entropies. This scaling behavior can be characterized by a trend of decreasing values of the respective entanglement measure for both early-times and around the quench point regions. Both scaling behaviors show thermalizing behavior of the respective entanglement measures at very late times.

(viii) It is quite clear from the plots that as we decrease the order of λ the value of both entanglement measures increases.

(ix) Also, for a given order of coupling constant λ von Neumann entropy thermalizes at higher values compared to that of Renyi entropy.

(x) Next we find that for a particular order of λ we obtain same scaling behavior for different orders of the Renyi entropy. However, the value of Renyi entropy decreases as we increase the order of Renyi entropy. The particular scaling behavior is retained

even for the case of very high order of Renyi entropy.

Future prospects:

(i) In the present article, we have analyzed the effects of quantum quench on the entanglement entropy for a system consisting of two coupled oscillators with quartic perturbation. Of course, this study of entanglement entropy and quantum quench can be generalized to that of N-coupled oscillators. For $N \to \infty$, in the continuous limit, it would be interesting to explore the effects of quantum quench on entanglement in the context of interacting field theory.

(ii) One of the latest developments in research in the field of high energy physics is, the study of circuit complexity [81–87]. There are some works which are focused on relating the complexity with quantum entanglement [79,88–91]. The study of the same might turn out to be intriguing in the case of interacting quenched field theories.

(iii) Hence, it would be interesting to explore the connection between quantum circuit complexity and entanglement and check its consistency with the CA and CV [92–95] proposal.

ACKNOWLEDGMENTS

APPENDIX A: COMPUTING EXPLICIT NUMERICAL VALUES OF $\sigma_i(T)$ AND $\gamma_i(T)$

Using auxiliary conditions given by Eq. (12) we briefly show the steps to compute σ_1 and γ_1. We begin by rearranging Eq. (12) for one of the oscillators,

$$\ddot{\sigma}_1 + \omega_1^2(T)\sigma_1 = \frac{\Omega_1}{\sigma_1^3}. \tag{A1}$$

The above second order differential equation is often termed as, Ermakov-Milne–Pinney equation [24–26]. This equation can be solved numerically to obtain $\sigma_1(T)$. Since $T = (t/\delta t)$, the solution will clearly be function of both t and δt. We assume that the form of solution of the above equation gives us a linear combination,

$$\sigma_1(t, \delta t) = c_1 z_1(t, \delta t) + c_2 z_2(t, \delta t). \tag{A2}$$

Here, c_1 and c_2 are numerical constants, while z_1 and z_2 are treated as two complex-valued solutions of Eq. (A1). We will consider only z_1 as one of the solutions. Using the form of quench profile Eq. (9), the computed value of one of the solutions is,

$$z_1(t, \delta t) = [e^{\frac{2t}{\delta t}}]^{-\frac{1}{2}(i\delta t)}[e^{\frac{2t}{\delta t}} + 1]^{\frac{1}{2}(\sqrt{1-4\delta t^2}+1)} {}_2F_1\left[\frac{1}{2}(\sqrt{1-4\delta t^2}+1), \frac{1}{2}(-2i\delta t + \sqrt{1-4\delta t^2}+1); 1 - i\delta t; -e^{\frac{2t}{\delta t}}\right]. \tag{A3}$$

Here, ${}_2F_1$ represents the hypergeometric function. Since z_1 is complex valued we can write, $z_1 = y_1 + iy_2$ such that y_1 and y_2 are now two real-linearly independent equations. We give an outline of steps shown in [96] for numerical solution of Eq. (A1) using these linearly independent equations. This solution is guaranteed to be of the form,

$$\sigma_1(t, \delta t) = [\sqrt{Ay_1^2(t, \delta t)t + 2By_1(t, \delta t)y_2(t, \delta t) + Cy_2^2(t, \delta t)}]. \tag{A4}$$

The next step is to determine the constants in Eq. (A4). These are fixed by setting the condition $AC - B^2 = \Omega_1^2$. These steps give us the explicit value of $\sigma_1(t, \delta t)$. One can repeat these steps by inserting the respective parameters (of second oscillator) to find $\sigma_2(t, \delta t)$. Since, $\Omega_i = \sigma_i^2 \dot{\gamma}_i$, the explicit value of γ_i is computed by using value of Eq. (A4),

$$\gamma_i(t, \delta t) = \int_0^t \frac{\Omega_i}{\sigma_i^2(t, \delta t)} dt \tag{A5}$$

Inserting the values of $\sigma_i(t, \delta t)$ and $\gamma_i(t, \delta t)$ it is clear that the wave function, in Eq. (23) becomes a function of both t and δt. Note that we conceal this functional dependence in all the sections until the entropy is numerically evaluated in Sec. V.

APPENDIX B: AN OUTLINE OF INVARIANT OPERATOR REPRESENTATION

In Sec. III we defined I_j as an operator in Eq. (14). We outline in this appendix a few important steps for constructing this operator and the way to find eigenstates of this operator. Note that the subscript $j = 1, 2$ represent the parameters described for the oscillators having spatial coordinates: X_1 and X_2 respectively.

The operator I_j is constructed such that it satisfies [18],

$$\frac{\partial I_j}{\partial T} + \frac{1}{i}[I_j, H_j], \tag{B1}$$

where H_j for $j = 1, 2$ represents the respective decoupled Hamiltonian for each oscillator (7). One can show that the operator given in Eq. (14) satisfies the above condition.

It is assumed that the invariant I_j is one of a complete set of commuting observables for respective H_j. This guarantees that there is a complete set of eigenstates for each I_j defined in Eq. (14). We refer to u_{0_j} for $j = 1, 2$ as the ground state for the spectrum of the respective invariant operator. These ground states of the respective invariant operators can be determined using the condition, $a_j u_{0_j} = 0$ where a_j is the respective annihilation operator Eq. (13). When evaluated, the expression for ground state of the invariant operator I_j is given by,

$$u_{0_j} = \left(\frac{\dot{\gamma}_j}{\pi}\right)^{1/4} \exp\left[-\frac{\dot{\gamma}_j}{2}(-i\dot{\sigma}_j \sigma_j \dot{\gamma}_j)X_j^2\right]. \tag{B2}$$

Using the ground states and the respective creation operators $a_j^\dagger$ one can then show that, the nth eigenstate of the invariant-operator I_j is given by,

$$u_{n_j} = \frac{1}{\sqrt{n!}}(a_j^\dagger)^n u_{0_j} = \left(\frac{1}{2^{n_j} n_j!}\right)\left(\frac{\dot{\gamma}_j}{\pi}\right)^{1/4}$$
$$\times \exp\left[\dot{\gamma}_j\left(1 - \frac{i\dot{\sigma}_j}{\sigma_j \dot{\gamma}_j}\right)X_j^2\right]\mathbf{H}_{n_j}\left[\sqrt{\dot{\gamma}_j}X_j\right]. \tag{B3}$$

Here, $j = 1, 2$ and $\mathbf{H}_{n_j}$ represents the Hermite polynomial of order n_j. Using the eigenstates of invariant operator (B3), one can compute the wave functions of the decoupled Hamiltonians [80]. It can be shown that the computed wave functions take the form: $\psi_{n_j} = e^{i\alpha_{n_j}} u_{n_j}$, as solutions to Schrodinger's equations for respective H_j, where $\alpha_{n_j} = -(1/2 + n_j)$; for $j = 1, 2$. The eigenstates for unperturbed Hamiltonian for the coupled oscillator system can further be computed as $\psi_{n_1,n_2}^{(0)} = \psi_{n_1} \times \psi_{n_2}$.

Using Eq. (B3) one can then show that,

$$\psi_{n_1,n_2}^{(0)} = \sqrt{\frac{\dot{\gamma}_1^2 \dot{\gamma}_1^2}{2^{n_1+n_2} n_1! n_2! \pi}} \exp\left[-i\frac{(2n_1+1)\gamma_1 + (2n_2+1)\gamma_2}{2}\right] \exp\left[-\frac{1}{2}\dot{\gamma}_1\left(-\frac{i\dot{\sigma}_1}{\dot{\gamma}_1 \sigma_1}\right)X_1^2 - \frac{1}{2}\dot{\gamma}_2\left(-\frac{i\dot{\sigma}_2}{\dot{\gamma}_2 \sigma_2}\right)X_2^2\right]$$
$$\times \mathbf{H}_{n_1}[\sqrt{\dot{\gamma}_1}X_1]\mathbf{H}_{n_2}[\sqrt{\dot{\gamma}_2}X_2]. \tag{B4}$$

This equation (B4) represents the eigenstates for the unperturbed Hamiltonian of two coupled oscillators having a quenched frequency profile. In III B we compute the first order time-independent correction to the ground state of above equation.

APPENDIX C: COMPUTING INTEGRALS IN $tr(\rho^n)$

In the integral of Eq. (32) we have separated both Gaussian and non-Guassian parts. In this appendix we give detailed outline of solving both Gaussian and non-Gaussian contributions and finally combine them to compute the integral in (32).

The Gaussian part of the integrand can be parametrized by considering a quadratic coefficient matrix similar to the case in [35]. Using the values of β_i for $i = 1$ to $i = 7$ defined in Sec. IV B, this coefficient matrix is defined as:

$$M_{ij} = -2(\beta_1 + \lambda\beta_2)\delta_{ij} - (\beta_3 + \lambda\beta_4)(\delta_{j+1}^i + \delta_j^{i+1}). \tag{C1}$$

We further modify the above defined matrix by introducing two new symbols μ and ξ. We choose these variables so that they satisfy,

$$\xi(1 + \mu^2) = -(\beta_1 + \lambda\beta_2)$$
$$2\xi\mu = \beta_3 + \lambda\beta_4. \tag{C2}$$

We consider the following explicit solution of these equations, approximated to first order in λ:

$$\mu = C_1 + \lambda C_2$$
$$\xi = C_3 + \lambda C_4. \tag{C3}$$

The values of newly defined coefficients $C_1, C_2 \ldots C_4$ are tabulated in Appendix D. Using matrix M_{ij} defined in Eq. (C1), one can recover the Gaussian part of Eq. (32) as shown below,

$$\exp\left[-\frac{1}{2}x^i M_{ij}x_j\right] = \exp\left[(\beta_1 + \lambda\beta_2)\sum_{i=1}^n x_i^2\right.$$
$$\left. + (\beta_3 + \lambda\beta_4)\sum_{i=1}^n x_i x_{i+1}\right]. \tag{C4}$$

Moving on to the non-Guassian part in Eq. (32), we further define a quartic tensor as:

$$T_{ijkl} = \lambda[\beta_5\delta_{ij}\delta_{jk}\delta_{kl} + (\alpha_7\delta_l^{k-1} + \alpha_6\delta_l^{k+1})\delta_{ij}\delta_{jk} + \beta_6\delta_{ij}\delta_k^{j+1}\delta_{kl}]. \tag{C5}$$

Using Eq. (C5), one can recover the remaining part of Eq. (32) as shown below,

$$\exp[x^i x^j x^k x^l T_{ijkl}] = \exp\left\{\lambda\left[\beta_5\sum_{i=1}^n x_i^4 + (\alpha_6 x_{i-1}^3 + \alpha_7 x_{i+1}^3)\sum_{i=1}^n x_i + \beta_6\sum_{i=1}^n x_i^2\sum_{i=1}^n x_{i+1}^2\right]\right\}. \tag{C6}$$

Using the expression shown in Eq. (C4) and the non-Gaussian contribution from Eq. (C6), one can parametrize the integrand in Eq. (32), as shown below:

$$tr(\rho^n) = N^n\left(\frac{g_1 g_2}{\pi}\right)^n\left(\sqrt{\frac{\pi}{A}}\right)^n e^{n(2\lambda A_1 + \lambda\alpha_0)}\int d^n x \exp\left[-\frac{1}{2}x^i M_{ij}x_j\right]\sum_{p=0}^\infty \frac{1}{i!}(x^i x^j x^k x^l T_{ijkl})^p. \tag{C7}$$

Further, we define a Gaussian partition function, Z_0, given by,

$$Z_0 = \int d^n x \exp\left[-\frac{1}{2}x^i M_{ij}x_j\right] = \sqrt{\frac{(2\pi)^n}{\det M}} = \frac{\left(\sqrt{\frac{\pi}{\xi}}\right)^n}{|1-\mu^n|}, \tag{C8}$$

where $\det M$ denotes the determinant of matrix M_{ij} of Eq. (C1). Using the above partition function the summed over tensor in Eq. (C7) can be transformed to a correlator as shown below retaining the form of perturbative expansion,

$$tr(\rho^n) = N^n\left(\frac{g_1 g_2}{\pi}\right)^n\left(\sqrt{\frac{\pi}{A}}\right)^n e^{n(2\lambda A_1 + \lambda\alpha_0)}Z_0\sum_{p=0}^\infty \frac{1}{p!}\langle\langle x^{i_1}x^{j_1}x^{k_1}x^{l_1}\ldots x^{i_p}x^{j_p}x^{k_p}x^{l_p}\rangle\rangle T_{i_1 j_1 k_1 l_1}\ldots T_{i_p j_p k_p l_p}. \tag{C9}$$

We simplify the above expression in Eq. (C9) using a generating functional J, as shown below,

$$Z(J) = \frac{1}{Z_0}\int d^n x \exp\left[-\frac{1}{2}x^i M_{ij}x_j + J_i x_i\right] = \exp\left[\frac{1}{2}J_i M_{ij}^{-1}J_j\right]. \tag{C10}$$

As shown in [35], correlator of Eq. (C9) computed using the above Eq. (C10) then becomes,

$$\langle\langle x_{i_1}\ldots xi_{2m}\rangle\rangle = \frac{\delta^{2m}}{\delta J_{i_1}\ldots\delta J_{i_{2m}}}Z(J)\Big|_{J=0} = \frac{1}{2^m m!}\sum_{\sigma\in S_G}(M^{-1})_{i_{\sigma(1)\sigma(2)}}\ldots(M^{-1})_{i_{\sigma(2n-1)\sigma(2n)}}. \tag{C11}$$

Here G is the quotient group which can be defined to reduce the sum significantly. Note that for a $4m$ point correlator function the chosen quotient group gives rise to three different permutations. A more detailed discussion about finding the quotient group G can be found in [35].

Using the value of quartic tensor from Eq. (C4) and the correlator from Eq. (C11), one can simplify Eq. (C9) as,

$$tr(\rho^n) = N^n Z_0\left(\frac{g_1 g_2}{\pi}\right)^n\left(\sqrt{\frac{\pi}{A}}\right)^n e^{n(2\lambda A_1 + \lambda\alpha_0)}\{1 + n\lambda[(3\beta_5 + \beta_6)(M_{11}^{-1})^2 + 3\beta_7 M_{11}^{-1}M_{12}^{-1} + 2\beta_6(M_{12}^{-1})^2]\}. \tag{C12}$$

One can check that the matrix inverses are [35],

$$M_{11}^{-1} = \frac{(\mu^{2n} - 1)}{2(1-\mu^n)^2\xi(\mu^2 - 1)}; \qquad M_{12}^{-1} = \frac{(\mu^n + \mu^2)}{2\mu\xi(\mu^2 - 1)(\mu^n - 1)}. \tag{C13}$$

APPENDIX D: TABULATED VALUES OF COEFFICIENTS

In this appendix, the values of various coefficients we have used in some steps to compute the analytical expression of entanglement measures, are tabulated in respective tables.

(i) We begin by listing the values of A_i for $i = 1, 2...6$ in Eq. (23) of Sec. III B in the table given below.

A_i	Coefficient of A_i
A_1	$\frac{3}{16}\left(-\frac{8\sigma_1^2\sigma_2^2}{\sigma_1^2\omega_1^2+\sigma_2^2\omega_2^2+\dot{\sigma}_1+\dot{\sigma}_2+\frac{1}{\sigma_1^2}+\frac{1}{\sigma_2^2}}+\frac{3\sigma_1^4+4\sigma_2^2\sigma_1^2}{\sigma_1^2\omega_1^2+\dot{\sigma}_1+\frac{1}{\sigma_1^2}}+\frac{3\sigma_2^4+4\sigma_1^2\sigma_2^2}{\sigma_2^2\omega_2^2+\dot{\sigma}_2+\frac{1}{\sigma_2^2}}\right)$
A_2	$\frac{3}{4}\sigma_1^2\left(\frac{4\sigma_2^2}{\sigma_1^2\omega_1^2+\sigma_2^2\omega_2^2+\dot{\sigma}_1+\dot{\sigma}_2+\frac{1}{\sigma_1^2}+\frac{1}{\sigma_2^2}}-\frac{\sigma_1^2+2\sigma_2^2}{\sigma_1^2\omega_1^2+\dot{\sigma}_1+\frac{1}{\sigma_1^2}}\right)$
A_3	or $\frac{3\sigma_1^2\sigma_2^2}{\sigma_1^2\omega_1^2+\sigma_2^2\omega_2^2+\dot{\sigma}_1+\dot{\sigma}_2+\frac{1}{\sigma_1^2}+\frac{1}{\sigma_2^2}}-\frac{3(\sigma_2^2+2\sigma_1^2\sigma_2^2)}{4(\sigma_2^2\omega_2^2+\dot{\sigma}_2+\frac{1}{\sigma_2^2})}$
A_4	$-\frac{\sigma_1^4}{4(\sigma_1^2\omega_1^2+\dot{\sigma}_1+\frac{1}{\sigma_1^2})}$
A_5	$-\frac{\sigma_2^4}{4(\sigma_2^2\omega_2^2+\dot{\sigma}_2+\frac{1}{\sigma_2^2})}$;
A_6	$-\frac{6\sigma_1^2\sigma_2^2}{\sigma_1^2\omega_1^2+\sigma_2^2\omega_2^2+\dot{\sigma}_1+\dot{\sigma}_2+\frac{1}{\sigma_1^2}+\frac{1}{\sigma_2^2}}$;

(ii) Next, we tabulate the values of coefficients α_i for $i = 1, 2...8$ in Eq. (28) of Sec. IV A.

α_i	Coefficient of α_i
α_0	$\frac{(A_2+A_3)}{2A}+\frac{3(A_4+A_5+A_6)}{8A^2}$
α_1	$\frac{(A_2+A_3)}{2}+\frac{(3A_4+3A_5-A_6)}{4A}+\frac{(A_2-A_3)(Q-P)}{2A}+\frac{(A_2+A_3)(Q-P)^2}{4A^2}+\frac{3(A_4-A_5)(Q-P)}{4A^2}+\frac{3(A_4+A_5+A_6)}{8A^3}(Q-P)^2$
α_2	$\frac{(A_2+A_3)}{2}+\frac{(3A_4+3A_5-A_6)}{4A}+\frac{(A_2-A_3)(Q^*-P^*)}{2A}+\frac{(A_2+A_3)(Q^*-P^*)^2}{4A^2}+\frac{3(A_4-A_5)(Q^*-P^*)}{4A^2}+\frac{3(A_4+A_5+A_6)}{8A^3}(Q^*-P^*)^2$
α_3	$\frac{(A_2-A_3)}{2A}(Q+Q^*-P-P^*)+\frac{(A_2+A_3)(Q-P)(Q^*-P^*)}{2A^2}+\frac{3(A_4-A_5)(Q+Q^*-P-P^*)}{4A_2}+\frac{3(A_4+A_5+A_6)(Q-P)(Q^*-P^*)}{4A^3}$
α_4	$\frac{(A_4+A_5+A_6)}{4}+\frac{(A_4-A_5)(Q-P)}{2A}+\frac{(3A_4+A_5-A_6)(Q-P)^2}{8A^2}+\frac{(A_4-A_5)(Q-P)^3}{8A^3}+\frac{(A_4+A_5+A_6)(Q-P)^4}{32A^4}$
α_5	$\frac{(A_4+A_5+A_6)}{4}+\frac{(A_4-A_5)(Q^*-P^*)}{2A}+\frac{(3A_4+A_5-A_6)(Q^*-P^*)^2}{8A^2}+\frac{(A_4-A_5)(Q^*-P^*)^3}{8A^3}+\frac{(A_4+A_5+A_6)(Q^*-P^*)^4}{32A^4}$
α_6	$\frac{(A_4-A_5)(Q^*-P^*)}{2A}+\frac{(3A_4+3A_5-A_6)(Q-P)(Q^*-p^*)}{4A^2}+\frac{(A_4-A_5)[3(Q-P)^2(Q^*-P^*)+(Q-P)^3]}{8A^3}+\frac{(A_4+A_5+A_6)(Q-P)^3(Q^*-P^*)}{8A^4}$
α_7	$\frac{(A_4-A_5)(Q-P)}{2A}+\frac{(3A_4+3A_5-A_6)(Q-P)(Q^*-p^*)}{4A^2}+\frac{(A_4-A_5)[3(Q-P)(Q^*-P^*)^2+(Q^*-P^*)^3]}{8A^3}+\frac{(A_4+A_5+A_6)(Q-P)(Q^*-P^*)^3}{8A^4}$
α_8	$\frac{(3A_4+3A_5-A_6)[(Q^*-P^*)^2+(Q-P)^2]}{8A^2}+\frac{(A_4-A_5)[3(Q-P)^2(Q^*-P^*)+3(Q-P)(Q^*-P^*)^2]}{8A^3}+\frac{(A_4+A_5+A_6)6(Q-P)^2(Q^*-P^*)^2}{32A^4}$

(iii) The values of β_i for $i = 1, 2...7$ in Eq. (32) of Sec. IV B are tabulated in the below given table.

β_i	Coefficient of β_i
β_1	$-A+\frac{(g_2^2-g_1^2)^2-(dg_1^2-fg_2^2)^2}{8A}$
β_2	$A_2+A_3+\frac{3A_4+3A_5-A_6}{2A}+\left(\frac{A_2-A_3}{2A}\right)(g_2^2-g_1^2)+\frac{3(A_4-A_5)(g_2^2-g_1^2)}{4A^2}+\left[\frac{3(A_4+A_5+A_6)}{16A^3}+\frac{A_2+A_3}{8A^2}\right][(g_2^2-g_1^2)^2-(dg_1^2-fg_2^2)^2]$
β_3	$\frac{(g_2^2-g_1^2)^2+(dg_1^2-fg_2^2)^2}{8A}$
β_4	$\left[\frac{A_2-A_3}{2A}+\frac{3(A_4-A_5)}{4A^2}\right][g_2^2-g_1^2]+\left[\frac{(A_2+A_3)}{8A^2}+\frac{3(A_4+A_5+A_6)}{16A^3}\right][(g_2^2-g_1^2)^2+(dg_1^2-fg_2^2)^2]$
β_5	$\frac{A_4+A_5+A_6}{2}+\frac{(A_4-A_5)(g_2^2-g_1^2)}{2A}+\frac{3A_4+3A_5-A_6}{16A^2}[(g_2^2-g_1^2)^2-(dg_1^2-fg_2^2)^2]+\frac{A_4-A_5}{64A^3}[2(g_2^2-g_1^2)^3-6(g_2^2-g_1^2)(dg_1^2-fg_2^2)^2]$ $+\frac{A_4+A_5+A_6}{512A^4}[2(g_2^2-g_1^2)^4+2(dg_1^2-fg_2^2)^4-12(g_2^2-g_1^2)^2(dg_1^2-fg_2^2)^2]$
β_6	$\left(\frac{3A_4+3A_5-A_6}{16A^2}\right)[(g_2^2-g_1^2)^2-(dg_1^2-fg_2^2)^2]+\left(\frac{3(A_4-A_5)}{32A^3}\right)[(g_2^2-g_1^2)^3+(g_2^2-g_1^2)(dg_1^2-fg_2^2)^2]+\left(\frac{6(A_4+A_5+A_6)}{512A^4}\right)[(g_2^2-g_1^2)^4$ $+(dg_1^2-fg_2^2)^4+2(g_2^2-g_1^2)^2(dg_1^2-fg_2^2)^2]$
β_7	$\frac{(A_4-A_5)(g_2^2-g_1^2)}{2A}+\left(\frac{3A_4+3A_5-A_6}{8A^2}\right)[(g_2^2-g_1^2)^2+(dg_1^2-fg_2^2)]+\left(\frac{A_4-A_5}{32A^3}\right)[(g_2^2-g_1^2)^3]+\left(\frac{A_4+A_5+A_6}{64A^4}\right)[(g_2^2-g_1^2)^4-(dg_1^2-fg_2^2)^4]$

(iv) The last table, given below contains values of C_i for $i = 1, 2, 3, 4$ in Eq. (C3) of Appendix C.

C_i	Value of C_i
C_1	$-\dfrac{\beta_1}{\beta_3} + \dfrac{(\beta_1^2 - \beta_3^2)^{\frac{1}{2}}}{\beta_3}$
C_2	$-\dfrac{\beta_2}{\beta_3} + \dfrac{(\beta_1\beta_2 - \beta_3\beta_4)}{\beta_3(\beta_1^2 - \beta_3^2)^{\frac{1}{2}}} + \dfrac{\beta_1\beta_4}{\beta_3^2} - \dfrac{\beta_4(\beta_1^2 - \beta_3^2)^{\frac{1}{2}}}{\beta_3^2}$
C_3	$\dfrac{\beta_3}{2C_1}$
C_4	$\dfrac{\beta_4}{2C_1} - \dfrac{C_2\beta_3}{2C_1^2}$

[1] P. Calabrese and J. Cardy, Entanglement entropy and quantum field theory, J. Stat. Mech. (2004) P06002.

[2] E. Witten, Notes on some entanglement properties of quantum field theory, Rev. Mod. Phys. **90,** 045003 (2018).

[3] T. Nishioka, Entanglement entropy: Holography and renormalization group, Rev. Mod. Phys. **90,** 035007 (2018).

[4] D. Blanco, Quantum information measures and their applications in quantum field theory, arXiv:1702.07384.

[5] M. Headrick, Lectures on entanglement entropy in field theory and holography, arXiv:1907.08126.

[6] L. Amico, R. Fazio, A. Osterloh, and V. Vedral, Entanglement in many-body systems, Rev. Mod. Phys. **80,** 517 (2008).

[7] J. I. Cirac, Entanglement in many-body quantum systems, arXiv:1205.3742.

[8] A. Lakshminarayan and V. Subrahmanyam, Multipartite entanglement in a one-dimensional time-dependent Ising model, Phys. Rev. A **71,** 062334 (2005).

[9] H. F. Song, S. Rachel, C. Flindt, I. Klich, N. Laflorencie, and K. Le Hur, Bipartite fluctuations as a probe of many-body entanglement, Phys. Rev. B **85,** 035409 (2012).

[10] C. J. Bardeen, Time dependent correlations of entangled states with nondegenerate branches and possible experimental realization using singlet fission, J. Chem. Phys. **151,** 124503 (2019).

[11] A. Sivaramakrishnan, Entanglement entropy with a time-dependent Hamiltonian, Phys. Rev. D **97,** 066003 (2018).

[12] P. Caputa, G. Mandal, and R. Sinha, Dynamical entanglement entropy with angular momentum and U(1) charge, J. High Energy Phys. 11 (2013) 52.

[13] E. Canovi, E. Ercolessi, P. Naldesi, L. Taddia, and D. Vodola, Dynamics of entanglement entropy and entanglement spectrum crossing a quantum phase transition, Phys. Rev. B **89,** 104303 (2014).

[14] P. Jacquod and C. Petitjean, Decoherence, entanglement and irreversibility in quantum dynamical systems with few degrees of freedom, Adv. Phys. **58,** 67 (2009).

[15] S. Akhtar, S. Choudhury, S. Chowdhury, D. Goswami, S. Panda, and A. Swain, Open quantum entanglement: A study of two atomic system in static patch of de Sitter space, Eur. Phys. J. C **80,** 748 (2020).

[16] S. Choudhury and S. Panda, Quantum entanglement in de Sitter space from stringy axion: An analysis using α vacua, Nucl. Phys. **B943,** 114606 (2019).

[17] S. Choudhury and S. Panda, Entangled de Sitter from stringy axionic Bell pair I: An analysis using Bunch–Davies vacuum, Eur. Phys. J. C **78,** 52 (2018).

[18] H. R. Lewis and W. B. Riesenfeld, An exact quantum theory of the time-dependent harmonic oscillator and of a charged particle in a time-dependent electromagnetic field, J. Math. Phys. (N.Y.) **10,** 1458 (1969).

[19] K. Andrzejewski, Dynamics of entropy and information of time-dependent quantum systems: Exact results, Quantum Inf. Process. **21,** 117 (2022).

[20] B. Khantoul, A. Bounames, and M. Maamache, On the invariant method for the time-dependent non-Hermitian Hamiltonians, Eur. Phys. J. Plus **132,** 258 (2017).

[21] S. Choudhury, Cosmological geometric phase from pure quantum states: A study without/with having Bell's inequality violation, arXiv:2105.06254.

[22] J.-R. Choi, Coherent and squeezed states for light in homogeneous conducting linear media by an invariant operator method, Int. J. Theor. Phys. **43,** 2113 (2004).

[23] H. Kanasugi and H. Okada, Systematic treatment of general time-dependent harmonic oscillator in classical and quantum mechanics, Prog. Theor. Phys. **93,** 949 (1995).

[24] V. P. Ermakov, Second-order differential equations: Conditions of complete integrability, *Applicable Analysis and Discrete Mathematics* (University of Belgrade, Serbia, 2008), pp. 123–145.

[25] W. Milne, The numerical determination of characteristic numbers, Phys. Rev. **35,** 863 (1930).

[26] E. Pinney, The nonlinear differential equation $y'' + p(x)y + cy^{-3} = 0$, Proc. Am. Math. Soc. **1,** 681 (1950).

[27] J. R. Choi, Perturbation theory for time-dependent quantum systems involving complex potentials, Front. Phys. **8,** 189 (2020).

[28] W. Wang, S. C. Hou, and X. X. Yi, Adiabatic evolution under quantum control, Ann. Phys. (Amsterdam) **327,** 1293 (2012).

[29] M.-Y. Ye, X.-F. Zhou, Y.-S. Zhang, and G.-C. Guo, Two kinds of quantum adiabatic approximation, Phys. Lett. A **368,** 18 (2007).

[30] K. Audenaert, J. Eisert, M. B. Plenio, and R. F. Werner, Entanglement properties of the harmonic chain, Phys. Rev. A **66,** 042327 (2002).

[31] A. Jafarizadeh and M. A. Rajabpour, Bipartite entanglement entropy of the excited states of free fermions and harmonic oscillators, Phys. Rev. B **100,** 165135 (2019).

[32] T. J. Osborne and M. A. Nielsen, Entanglement in a simple quantum phase transition, Phys. Rev. A **66,** 032110 (2002).

[33] R. D. Sorkin, Expressing entropy globally in terms of (4D) field-correlations, J. Phys. Conf. Ser. **484,** 012004 (2014).

[34] C. Holzhey, F. Larsen, and F. Wilczek, Geometric and renormalized entropy in conformal field theory, Nucl. Phys. **B424,** 443 (1994).

[35] Y. Chen, L. Hackl, R. Kunjwal, H. Moradi, Y. K. Yazdi, and M. Zilhão, Towards spacetime entanglement entropy for interacting theories, J. High Energy Phys. 11 (2020) 114.

[36] V. Rosenhaus and M. Smolkin, Entanglement entropy: A perturbative calculation, J. High Energy Phys. 12 (2014) 179.

[37] P. Calabrese and J. Cardy, Quantum quenches in extended systems, J. Stat. Mech. (2007) P06008.

[38] P. Basu and S. R. Das, Quantum quench across a holographic critical point, J. High Energy Phys. 01 (2012) 103.

[39] A. Buchel, L. Lehner, R. C. Myers, and A. van Niekerk, Quantum quenches of holographic plasmas, J. High Energy Phys. 05 (2013) 067.

[40] S. R. Das, D. A. Galante, and R. C. Myers, Universal Scaling in Fast Quantum Quenches in Conformal Field Theories, Phys. Rev. Lett. **112,** 171601 (2014).

[41] S. R. Das, D. A. Galante, and R. C. Myers, Universality in fast quantum quenches, J. High Energy Phys. 02 (2015) 167.

[42] S. R. Das, D. A. Galante, and R. C. Myers, Smooth and fast versus instantaneous quenches in quantum field theory, J. High Energy Phys. 08 (2015) 073.

[43] S. R. Das, D. A. Galante, and R. C. Myers, Quantum quenches in free field theory: Universal scaling at any rate, J. High Energy Phys. 05 (2016) 164.

[44] V. Alba and P. Calabrese, Entanglement dynamics after quantum quenches in generic integrable systems, SciPost Phys. **4,** 017 (2018).

[45] S. Ghosh, K. S. Gupta, and S. C. L. Srivastava, Entanglement dynamics following a sudden quench: An exact solution, Europhys. Lett. **120,** 50005 (2017).

[46] S. Ghosh, K. S. Gupta, and S. C. L. Srivastava, Exact relaxation dynamics and quantum information scrambling in multiply quenched harmonic chains, Phys. Rev. E **100,** 012215 (2019).

[47] A. Polkovnikov, K. Sengupta, A. Silva, and M. Vengalattore, Colloquium: Nonequilibrium dynamics of closed interacting quantum systems, Rev. Mod. Phys. **83,** 863 (2011).

[48] C. Gogolin and J. Eisert, Equilibration, thermalisation, and the emergence of statistical mechanics in closed quantum systems, Rep. Prog. Phys. **79,** 056001 (2016).

[49] P. Calabrese, F. H. L. Essler, and G. Mussardo, Introduction to 'quantum integrability in out of equilibrium systems', J. Stat. Mech. (2016) 064001.

[50] T. Langen, T. Gasenzer, and J. Schmiedmayer, Prethermalization and universal dynamics in near-integrable quantum systems, J. Stat. Mech. (2016) 064009.

[51] T. Kinoshita, T. Wenger, and D. Weiss, A quantum Newton's cradle, Nature (London) **440,** 900 (2006).

[52] S. Hofferberth, I. Lesanovsky, B. Fischer, T. Schumm, and J. Schmiedmayer, Non-equilibrium coherence dynamics in one-dimensional Bose gases, Nature (London) **449,** 324 (2007).

[53] S. Trotzky, Y. A. Chen, A. Flesch, I. P. McCulloch, U. Schollwöck, J. Eisert, and I. Bloch, Probing the relaxation towards equilibrium in an isolated strongly correlated one-dimensional Bose gas, Nat. Phys. **8,** 325 (2012).

[54] M. Gring, M. Kuhnert, T. Langen, T. Kitagawa, B. Rauer, M. Schreitl, I. Mazets, D. A. Smith, E. Demler, and J. Schmiedmayer, Relaxation and prethermalization in an isolated quantum system, Science **337,** 1318 (2012).

[55] M. Cheneau, P. Barmettler, D. Poletti, M. Endres, P. Schauß, T. Fukuhara, C. Gross, I. Bloch, C. Kollath, and S. Kuhr, Light-cone-like spreading of correlations in a quantum many-body system, Nature (London) **481,** 484 (2012).

[56] F. Meinert, M. J. Mark, E. Kirilov, K. Lauber, P. Weinmann, A. J. Daley, and H.-C. Nägerl, Quantum Quench in an Atomic One-Dimensional Ising Chain, Phys. Rev. Lett. **111,** 053003 (2013).

[57] T. Langen, R. Geiger, M. Kuhnert, B. Rauer, and J. Schmiedmayer, Local emergence of thermal correlations in an isolated quantum many-body system, Nat. Phys. **9,** 640 (2013).

[58] T. Fukuhara, P. Schauß, M. Endres, S. Hild, M. Cheneau, I. Bloch, and C. Gross, Microscopic observation of magnon bound states and their dynamics, Nature (London) **502,** 76 (2013).

[59] T. Fukuhara, A. Kantian, M. Endres, M. Cheneau, P. Schauß, S. Hild, D. Bellem, U. Schollwöck, T. Giamarchi, C. Gross, I. Bloch, and S. Kuhr, Quantum dynamics of a mobile spin impurity, Nat. Phys. **9,** 235 (2013).

[60] S. Sotiriadis and J. Cardy, Quantum quench in interacting field theory: A self-consistent approximation, Phys. Rev. B **81,** 134305 (2010).

[61] D. Han, Y. Kim, and M. Noz, Illustrative example of Feynman's rest of the universe, Am. J. Phys. **67,** 61 (1999).

[62] J. S. Prauzner-Bechcicki, Two-mode squeezed vacuum state coupled to the common thermal reservoir, J. Phys. A **37,** L173 (2004).

[63] D. Han, Y. S. Kim, and M. E. Noz, Linear canonical transformations of coherent and squeezed states in the wigner phase space. iii. two-mode states, Phys. Rev. A **41,** 6233 (1990).

[64] Y. S. Kim, Observable Gauge Transformations in the Parton Picture, Phys. Rev. Lett. **63,** 348 (1989).

[65] F. Iachello and S. Oss, Model of *n* Coupled Anharmonic Oscillators and Applications to Octahedral Molecules, Phys. Rev. Lett. **66,** 2976 (1991).

[66] S. Ikeda and F. Fillaux, Incoherent elastic-neutron-scattering study of the vibrational dynamics and spin-related symmetry of protons in the khco$_3$ crystal, Phys. Rev. B **59**, 4134 (1999).

[67] F. Fillaux, Quantum entanglement and nonlocal proton transfer dynamics in dimers of formic acid and analogues, Chem. Phys. Lett. **408**, 302 (2005).

[68] M. Delor, S. Archer, T. Keane, A. Meijer, I. Sazanovich, G. Greetham, M. Towrie, and J. Weinstein, Directing the path of light-induced electron transfer at a molecular fork using vibrational excitation, Nat. Chem. **9**, 1099 (2017).

[69] E. Romero, R. Augulis, V. Novoderezhkin, M. Ferretti, J. Thieme, D. Zigmantas, and R. van Grondelle, Quantum coherence in photosynthesis for efficient solar energy conversion, Nat. Phys. **10**, 676 (2014).

[70] F. D. Fuller, J. Pan, A. Gelzinis, V. Butkus, S. S. Senlik, D. E. Wilcox, C. F. Yocum, L. Valkunas, D. Abramavicius, and J. P. Ogilvie, Vibronic coherence in oxygenic photosynthesis, Nat. Chem. **6**, 706 (2014).

[71] A. Halpin, P. Johnson, R. Tempelaar, R. Murphy, J. Knoester, T. Jansen, and R. Miller, Two-dimensional spectroscopy of a molecular dimer unveils the effects of vibronic coupling on exciton coherences, Nat. Chem. **6**, 196 (2014).

[72] D. N. Makarov, Coupled harmonic oscillators and their quantum entanglement, Phys. Rev. E **97**, 042203 (2018).

[73] J.-Y. Kao and C.-H. Chou, Quantum entanglement in coupled harmonic oscillator systems: From micro to macro, New J. Phys. **18**, 073001 (2016).

[74] A. Jellal, F. Madouri, and A. Merdaci, Entanglement in coupled harmonic oscillators studied using a unitary transformation, J. Stat. Mech. (2011) P09015.

[75] M. S. Abdalla, M. Abdel-Aty, and A.-S. F. Obada, Degree of entanglement for anisotropic coupled oscillators interacting with a single atom, J. Opt. B **4**, 396 (2002).

[76] M. B. Plenio, J. Hartley, and J. Eisert, Dynamics and manipulation of entanglement in coupled harmonic systems with many degrees of freedom, New J. Phys. **6**, 36 (2004).

[77] R. A. Jefferson and R. C. Myers, Circuit complexity in quantum field theory, J. High Energy Phys. 10 (2017) 107.

[78] P. Caputa, S. R. Das, M. Nozaki, and A. Tomiya, Quantum quench and scaling of entanglement entropy, Phys. Lett. B **772**, 53 (2017).

[79] H. A. Camargo, P. Caputa, D. Das, M. P. Heller, and R. Jefferson, Complexity as a Novel Probe of Quantum Quenches: Universal Scalings and Purifications, Phys. Rev. Lett. **122**, 081601 (2019).

[80] K. H. Yeon, H. J. Kim, C. I. Um, T. F. George, and L. N. Pandey, Wave function in the invariant representation and squeezed-state function of the time-dependent harmonic oscillator, Phys. Rev. A **50**, 1035 (1994).

[81] K. Adhikari, S. Choudhury, S. Kumar, S. Mandal, N. Pandey, A. Roy, S. Sarkar, P. Sarker, and S. S. Shariff, Circuit complexity in $\mathcal{Z}_2\mathcal{EEFT}$, arXiv:2109.09759.

[82] K. Adhikari, S. Choudhury, and A. Roy, Krylov complexity in quantum field theory, arXiv:2204.02250.

[83] K. Adhikari, S. Choudhury, H. N. Pandya, and R. Srivastava, PGW circuit complexity, arXiv:2108.10334.

[84] S. Choudhury, A. Mukherjee, N. Pandey, and A. Roy, Causality constraint on circuit complexity from $\mathcal{COSMOEFT}$, arXiv:2111.11468.

[85] K. Adhikari and S. Choudhury, Cosmological krylov complexity, arXiv:2203.14330.

[86] P. Bhargava, S. Choudhury, S. Chowdhury, A. Mishara, S. P. Selvam, S. Panda, and G. D. Pasquino, Quantum aspects of chaos and complexity from bouncing cosmology: A study with two-mode single field squeezed state formalism, SciPost Phys. Core **4**, 026 (2021).

[87] R. A. Jefferson and R. C. Myers, Circuit complexity in quantum field theory, J. High Energy Phys. 10 (2017) 107.

[88] K. Adhikari, S. Choudhury, S. Chowdhury, K. Shirish, and A. Swain, Circuit complexity as a novel probe of quantum entanglement: A study with black hole gas in arbitrary dimensions, Phys. Rev. D **104**, 065002 (2021).

[89] S. Choudhury, S. Chowdhury, N. Gupta, A. Mishara, S. P. Selvam, S. Panda, G. D. Pasquino, C. Singha, and A. Swain, Circuit complexity from cosmological Islands, Symmetry **13**, 1301 (2021).

[90] J. Eisert, Entangling Power and Quantum Circuit Complexity, Phys. Rev. Lett. **127**, 020501 (2021).

[91] S. D. Mathur, Three puzzles in cosmology, Int. J. Mod. Phys. D **29**, 2030013 (2020).

[92] D. Stanford and L. Susskind, Complexity and shock wave geometries, Phys. Rev. D **90**, 126007 (2014).

[93] L. Susskind, Addendum to computational complexity and black hole horizons, Fortschr. Phys. **64**, 24 (2016).

[94] D. A. Roberts, D. Stanford, and L. Susskind, Localized shocks, J. High Energy Phys. 03 (2015) 051.

[95] L. Susskind and Y. Zhao, Switchbacks and the bridge to nowhere, arXiv:1408.2823.

[96] S. Mukherjee, A. Ghose Choudhury, and P. Guha, Generalized damped Milne-Pinney equation and Chiellini method, arXiv:1603.08747.